

Rubber-Modified Glassy Amorphous Polymers Prepared via Chemically Induced Phase Separation. 4. Comparison of Properties of Semi- and Full-IPNs, and Copolymers of Acrylate–Aliphatic Epoxy Systems

B. J. P. Jansen, S. Rastogi, H. E. H. Meijer,* and P. J. Lemstra

Eindhoven Polymer Laboratories, The Dutch Polymer Institute, Eindhoven University of Technology, PO Box 513, 5600 MB Eindhoven, The Netherlands

Received September 4, 1998; Revised Manuscript Received March 22, 1999

ABSTRACT: The introduction of rubbery particles can be applied to enhance shear yielding and, consequently, the toughness of brittle amorphous polymers. The critical transition in these polymers from crazing to shear yielding requires a submicrometer- or even nanometer-sized rubbery phase. These can be obtained via coalescence suppression in processes involving chemically induced phase separation but are also obtained in interpenetrating polymer networks (IPN) where cross-linking or gelation is responsible for the morphology control. In all cases, the formation of a nanometer-sized morphology is accompanied by an enhanced interphase mixing, i.e., incomplete demixing resulting in a broad interface in which the composition gradually changes from one phase to the other. In this study, the influence of interphase mixing on the mechanical properties has been investigated. Besides the standard semi-IPN system based on poly(methyl methacrylate) and aliphatic epoxy resins, two additional systems being composed of the same constituents but with an increased degree of interfacial mixing have been investigated: a full-IPN prepared by cross-linking the acrylate phase and a copolymer system in which the acrylate phase is chemically bonded to the epoxy phase. In situ small-angle X-ray scattering experiments during tensile deformation demonstrated that the microscopic deformation mechanism is clearly influenced by the degree of demixing. Despite this, the macroscopic toughness is found to be rather system independent since for all three systems, a comparable synergistic toughening effect is observed in both tensile and impact deformation.

1. Introduction

In previous papers, a fundamental approach toward toughening of brittle amorphous polymers has been discussed.^{1–5} One of the results of these studies was that toughening can be accomplished by making the material locally extremely thin via the introduction of a submicrometer- or even nanometer-sized rubbery dispersed phase. Since these morphologies cannot be prepared via conventional blending techniques, an alternative blending route has been explored which involves chemically induced phase separation during the in situ polymerization of an initially homogeneous monomer solution.⁶ This method is used to prepare a blend of poly(methyl methacrylate) (PMMA) with a dispersed rubbery epoxy phase, whose size is tailored by controlling the coarsening process after phase separation.

The morphology obtained, and its preparation route, is comparable to that of interpenetrating polymer networks (IPN).^{7,8} IPNs are defined as a combination of two or more polymer networks, with at least one of them polymerized and/or cross-linked in the immediate presence of the other(s).⁹ Initially, IPNs were considered as quasi-homogeneous; however, in most systems microscopic phase separation occurs sometimes on a scale of tens of nanometers only.^{10,11} In some cases, these morphologies can indeed yield unique mechanical properties. Examples are IPNs of polymethacrylates with polyurethane^{12–16} or siloxanes,¹⁷ and poly(ethylene terephthalate) with castor oil,¹⁸ which all can possess, for certain compositions, an extremely high strain at break. The fundamental explanation for these apparent improvements in mechanical properties is, however, still lacking and hardly any attention is paid to relation between the morphology and the mode of microscopic

deformation.¹⁹ The objective of this paper is to, at least partly, reveal some of the relevant mechanisms.

Generally, two types of IPNs are distinguished: full-IPNs in which all networks are cross-linked and semi-IPNs in which at least one thermoplastic phase is present. The nanometer-sized morphologies of certain full-IPNs are a direct result of cross-linking, which can suppress the coarsening process during polymerization and phase separation. This approach can also be used to accomplish the same morphology size in semi-IPNs in which the cross-linked polymer forms the matrix. Morphology control in semi-IPNs in which a thermoplastic matrix is desired will be much more difficult since the cross-linked polymer is produced in the presence of or after the formation of the thermoplastic phase. As a result, cross-linking cannot be used to suppress morphology coarsening during phase separation which results in a micrometer- rather than nanometer-sized morphology, as observed in PPE/epoxy²⁰ and PEI/epoxy.²¹ Therefore, this obvious route cannot be chosen as the optimal one in the preparation of our PMMA/epoxy blends, which indeed can be classified as semi-IPNs. Alternatively, it is possible to obtain specific morphologies in semi-IPNs by controlling the coarsening process after phase separation via the system viscosity.^{1,6} However, like cross-linking, an enhanced viscosity can also suppress the degree of demixing.

Nevertheless, it is of interest to study the influence of interphase mixing on the mechanical properties in order to elucidate the mechanisms of the enhanced toughness phenomena as observed for the previously investigated PMMA/epoxy, semi-IPNs system.¹ Therefore, three systems were designed: besides the mentioned semi-IPN of PMMA/epoxy,¹ a full-IPN, obtained

by cross-linking of the PMMA phase, and a copolymer prepared by using the same constituents. The differences in mechanical behavior on both the macroscopic and microscopic levels are studied.

2. Experimental Section

2.1. Materials. The epoxy resin used is a diglycidyl ether of poly(propylene oxide) (DGEPO, SHELL Epikote 877) supplied by CFZ (Chemische Fabriek Zaltbommel, Zaltbommel, The Netherlands). The curing agent, Jeffamine D230 supplied by Huntsman (Zaventem, Belgium), is a diamine which also possesses a poly(propylene oxide) (PPO) backbone.

In the free-radical polymerization, several monomers were used: methyl methacrylate (MMA, Aldrich), diethylene glycol dimethacrylate (DEGDMA, Aldrich) and glycidyl methacrylate (GMA, Aldrich). All monomers were purified prior to use. The polymerization was performed over a broad temperature range which required the application of three initiators with different reactivity: 2,2'-azobis(4-methoxy-2,4-dimethylvaleronitrile) (V-70 initiator supplied by WAKO Chemicals, Neuss, Germany), 2,2'-azobis(isobutyronitrile) (Perkadox AIBN, AKZO-NOBEL) and *tert*-butyl peroxybenzoate (Aldrich). The 10 h half-life time decomposition temperature in toluene of these initiators increases, respectively, from 30 and 64 to 103 °C.

2.2. Blend Preparation. The polymerization of MMA and epoxy was performed simultaneously and was similar to the procedure described in part 1 of this series.¹ A homogeneous solution of MMA, epoxy, curing agent, and the three mentioned free-radical initiators was prepared for several MMA-epoxy weight ratios. After the solution was purged with nitrogen gas for several minutes, the polymerization was performed in a closed cast mold. Immediately after the addition of the most reactive initiator, V-70, the polymerization of MMA was initiated. The solution was left at room temperature for 24 h. Subsequently, the molds were placed in an oven with a programmed temperature profile: 20 h at, subsequently, 30, 50, 70, and 90 °C, followed by two post-curing steps at 110 °C for 3 h and 120 °C for 2 h. Afterward, the molds were kept in the oven, which was allowed to cool slowly to room temperature.

The blends obtained consist of a thermoplastic PMMA matrix with a dispersed epoxy rubber phase.¹ Considering the simultaneous polymerization route and the character of the phases, these blends can be classified as semi-IPNs. The same route was followed to prepare full-IPNs and copolymers based on the constituents mentioned above. The recipe involved the addition of, respectively, DEGDMA (6.5 wt % based on MMA), as a cross-linking agent for the PMMA phase, or GMA (12.2 wt % based on Epikote 877), which participates in both the MMA free-radical and the epoxy step polymerizations.²²

2.3. Analysis. Dynamic mechanical thermal analysis (DMTA) was performed for all blends prepared. A Polymer Laboratories (now: Rheometrics Scientific) Dynamic Mechanical Thermal Analyzer MkII was used in the bending mode with a frequency of 1 Hz, a strain of 40 μ m, and a heating rate of 2 °C/min.

Transmission (TEM, JEOL 2000 FX) electron microscopy was used to investigate the morphology of the blends. The samples were microtomed below their glass transition temperature using a Reichert-Jung Ultracut E. Contrast was enhanced by staining the epoxy phase using RuO₄ vapor for 10 min.

2.4. Mechanical Properties. Tensile tests were performed at room temperature using a Zwick 1445 tensile machine. Dog-bone-shaped tensile bars with a gauge length of 38 mm were machined from the polymerized plaques and tested at a strain rate of 1.3×10^{-3} s⁻¹. An Instron Extensometer 2630-107 was used to collect accurate displacement data to determine the blend moduli.

Impact tensile tests (1 m/s) were performed using a Zwick Rel SB 3122 tensile machine. The test specimens were prepared according to the ASTM D-256 protocol. However, in this case the machined notches were sharpened prior to testing using a fresh razor blade. The impact energy was calculated

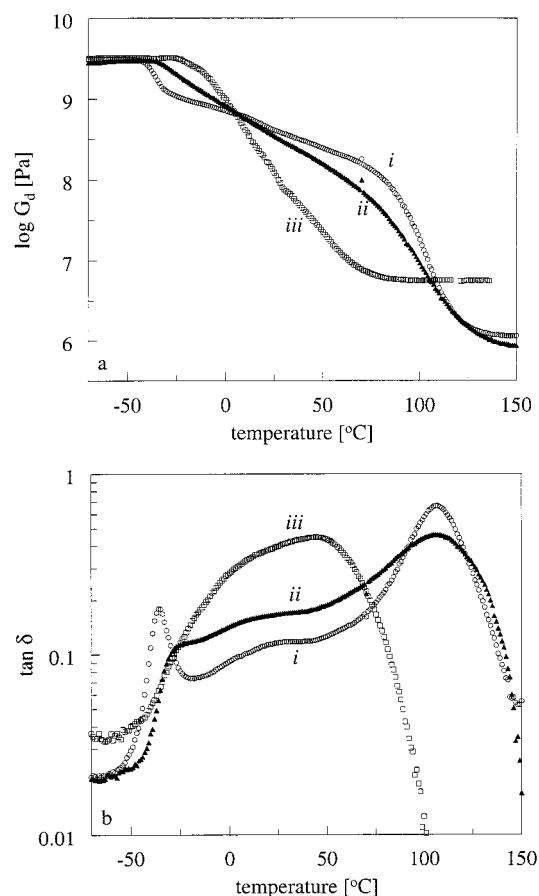


Figure 1. DMTA measurements of in situ polymerized PMMA/epoxy 50/50 blends, of (a) dynamic modulus ($\log G_d$) and (b) loss angle ($\tan \delta$): (i) semi-IPN; (ii) full-IPN; (iii) GMA copolymer.

by the integration of the measured force-displacement curve divided by the fracture surface area.

2.5. Microscopic Deformation. The microscopic deformation mechanism during tensile deformation is studied by time-resolved small-angle X-ray experiments using the synchrotron radiation facility at the ESRF (European Synchrotron Radiation Facilities, Grenoble, France). The measurements were performed at beamline ID2-BL4 using a X-ray wavelength of 1 Å and a detector-to-sample distance of 10 m. The size of the beam was 0.2×0.5 mm². For all three systems, samples of the 90/10, 80/20, and 70/30 compositions were deformed in uniaxial tension using a Rheometrics Minimat miniature tensile machine at a displacement rate of 0.1 mm/min. The scattering patterns were collected using a 2D-CCD detector. The patterns were used for the qualitative identification of the mode of microscopic deformation.

3. Results and Discussion

3.1. DMTA Measurements. The influences on demixing are studied by DMTA measurements, as shown for the PMMA/epoxy 50/50 blends in Figure 1. For the semi-IPN, clearly two peaks and thus two separate phases are obtained. By cross-linking the PMMA phase, the degree of demixing is decreased, as can be concluded from the suppression of the rubber transition at ~ -35 °C, and the enhanced broadening of the PMMA transition. For the GMA copolymer, $\tan \delta$ gives only one very broad peak, bridging the temperature range from the epoxy T_g (~ -35 °C) to the T_g of the PMMA phase (~ 115 °C). The dynamic modulus G_d does not show any transitions but slowly falls off in the same temperature range. This suggests the presence of one single copoly-

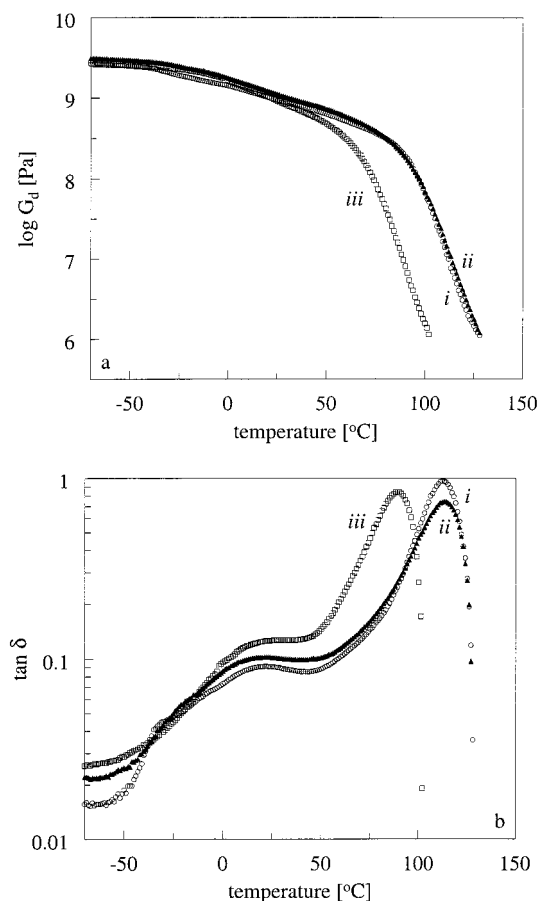


Figure 2. DMTA measurements of in situ polymerized PMMA/epoxy 80/20 blends, of (a) dynamic modulus ($\log G_d$) and (b) loss angle ($\tan \delta$): (i) semi-IPN; (ii) full-IPN; (iii) GMA copolymer.

mer phase, despite the fact that this behavior is clearly different from that of a completely statistical random copolymer where one single, sharp, peak is observed at a glass transition temperature determined by the ratio of the constituents. The DMTA data of the GMA copolymer suggests a more quasi-homogeneous network possessing a broad spectrum of compositions which include all intermediate ratios between neat PMMA and epoxy. As expected, the effects observed in DMTA are less pronounced for blends in which one of both phases is present in excess; see, e.g., the PMMA/epoxy 80/20 blend in Figure 2. The differences resulting from demixing can, however, still be observed and may thus affect the mechanical behavior.

3.2. Morphology. The trends in demixing observed in the DMTA measurements are confirmed by the morphology studies, see Figure 3, and the optical appearance of the blends, see Table 1. For the GMA copolymer, all compositions are transparent while some of the full- and semi-IPNs are white due to a relatively coarse two-phase morphology. The composition at which the blends become hazy, increases from 50 wt % epoxy for the semi-IPN to 60–70 wt % for the full-IPN. Apparently, the size of the morphology decreases as the PMMA phase is cross-linked or even chemically bonded

to the epoxy phase which is confirmed by the TEM micrographs in Figure 3.

3.3. Tensile Behavior. Surprisingly, the macroscopic strain at break seems to be hardly affected by the huge differences in demixing or morphology, see Figure 4. All three blends show a comparable synergistic effect with a high strain at break for the intermediate epoxy concentrations. The only real difference is observed at epoxy concentrations in the range 40–70 wt % where the strain at break of the GMA copolymer system is found to decrease more rapidly in comparison to both IPNs. This is most likely the result of the high cross-link-density of GMA copolymer.

For a low epoxy content the differences in the “so-called” plastic strain at break are also limited. The plastic strain at break is defined by the ratio between the cross-sectional area before and after fracture and supplies some information about the relative amount of plastic deformation compared to elastic deformation and thus the contribution of the rubber phase. The GMA copolymer systems appear to be almost completely elastic for blends containing 50 wt % epoxy or more. In comparison, the semi- and full-IPNs deform much more plastically, also at intermediate epoxy concentrations. Compared to the semi-IPN, the plastic strain at break of the full-IPN is smaller, which is most probably the result of cross-linking in combination with an enhanced elasticity (reflected by a high reversible deformation) as result of a decreased demixing.

Apart from the (minor) differences described above, the strain at break data, although spectacular for PMMA, suggest a rather uniform overall deformation behavior for all three systems. However, the more detailed stress–strain behavior of the 60/40 compositions in Figure 5a, as an example of three distinct experiments, clearly shows that there is a considerable influence of demixing. The semi-IPNs demonstrate a clear yield stress followed by pronounced strain softening known from the tensile and compression behavior of blends consisting of rubber particles in thermoplastic matrixes. For both the full-IPN and the copolymer, however, the yield stress is suppressed and the strain softening is completely disappeared. This clearly shows that decreasing the degree of demixing enhances the influence of the epoxy rubber phase. As can be expected, this effect is less pronounced for systems with a higher PMMA content which all demonstrate a stress–strain behavior with a clear yield stress followed by strain softening; see Figure 5b for three distinct experiments for the 80/20 composition. However, the values of the yield stress and modulus for the full-IPNs and the GMA copolymers are somewhat smaller compared to the blendlike semi-IPNs, see Figure 6 which shows the average of at least five experiments.

3.4. Tensile and Impact Toughness. In slow speed tensile testing, modulus, yield stress, and strain at break can be combined to a definition of tensile toughness, through the absorbed energy during tensile deformation till fracture, represented by the area under the stress–strain curve. For low epoxy contents (<20 wt %) limited differences are observed; see Figure 7a.

Table 1. Optical Appearance of the PMMA/Epoxy Blends

PMMA/epoxy	90/10	80/20	70/30	60/40	50/50	40/60	30/70	20/80	10/90
semi-IPN		transparent			hazy		white		transparent
full-IPN			transparent			hazy		white	transparent
copolymer					transparent				

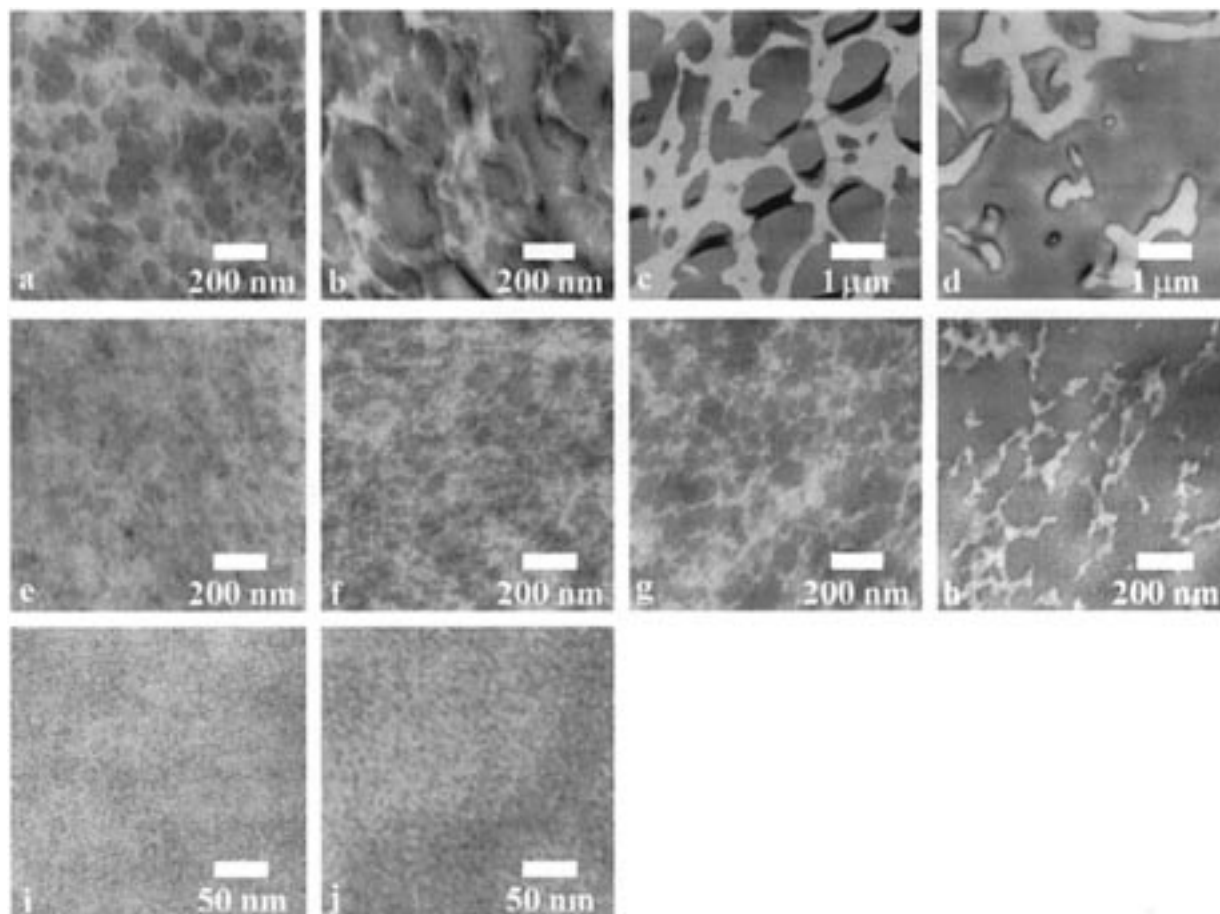


Figure 3. Transmission electron micrographs of the PMMA/epoxy systems: semi-IPNs, (a) 50/50, (b) 40/60, (c) 30/70, and (d) 20/80; (e–h) same compositions for the full-IPNs; copolymer (i) 50/50, and (j) 20/80.

For higher epoxy contents, the tensile toughness of the semi-IPNs is clearly larger as a result of the higher strain at break in combination with the higher yield stress and modulus. The rapidly decreasing toughness of the GMA copolymer is explained by the almost totally elastic behavior of this system.

Under notched impact conditions a comparable trend in toughness can be expected. However, the rubber content at which the maximum toughness is now observed, clearly shifts to higher values (compare parts a and b of Figure 7). Apparently, the strain rate dependence of toughness is not really affected by the degree of interphase mixing since its absolute value is rather system independent. The full-IPN and GMA copolymer demonstrate a somewhat remarkable trend for epoxy concentrations less than 50 wt %. In contrast to the concentration independent behavior of the semi-IPNs, the toughness appears to decrease with increasing rubber content. This is most likely again the result of the more elastic behavior of the systems with a higher rubber content and the absence of a separate rubber phase which results in an enhanced notch sensitivity.^{1,3} In part 3 of this series, it was demonstrated that precavitating the PMMA/epoxy 80/20 blend in tension prior to impact testing resulted in a significant enhancement of the impact toughness, even at low epoxy concentrations.³ In general, the toughness of the blends is mainly determined by these kind of microscopic deformation phenomena which may be influenced by the degree of interphase mixing as will be discussed in more detail in the following section.

3.5. Mode of Microscopic Deformation. Despite the limited difference in macroscopic mechanical behavior, the deformation on a microscopic level may still be affected by the degree of demixing. As in the previous papers, time-resolved SAXS is used to monitor the mode of microscopic deformation.^{2,3} The resulting scattering patterns prior to fracture as shown in Figure 8 are used for the qualitative identification of the microscopic deformation.

3.5.1. Semi-IPNs. The mode of microscopic deformation of the semi-IPNs, as shown in Figure 8a–c, have extensively been discussed before.² For the 90/10 blend, the strong scattering streaks in the tensile direction in combination with the weaker scattering perpendicular to that, have been explained by the introduction of crazes; see Figure 8a. During the early stage of the drawing process of the 80/20 blend, voids are formed as result of rubber cavitation. The elliptical scattering pattern in a later stage, see Figure 8b, is caused by the elongation of these voids in the tensile direction. Deformation of this blend occurs via shear yielding which explains the enhanced tensile toughness on macroscopic level. Finally, the 70/30 blend also deforms via shear yielding, however, without the formation of voids. The observed scattering pattern is caused by the orientation of the rubber morphology upon drawing; see Figure 8c.

3.5.2. Full-IPNs. The scattering patterns for the full-IPN are shown in Figure 8d–f. The brittle 90/10 system again deforms via crazing as can be concluded from the strong scattering streaks in the tensile direction; see Figure 8d. No relevant scattering is observed in the

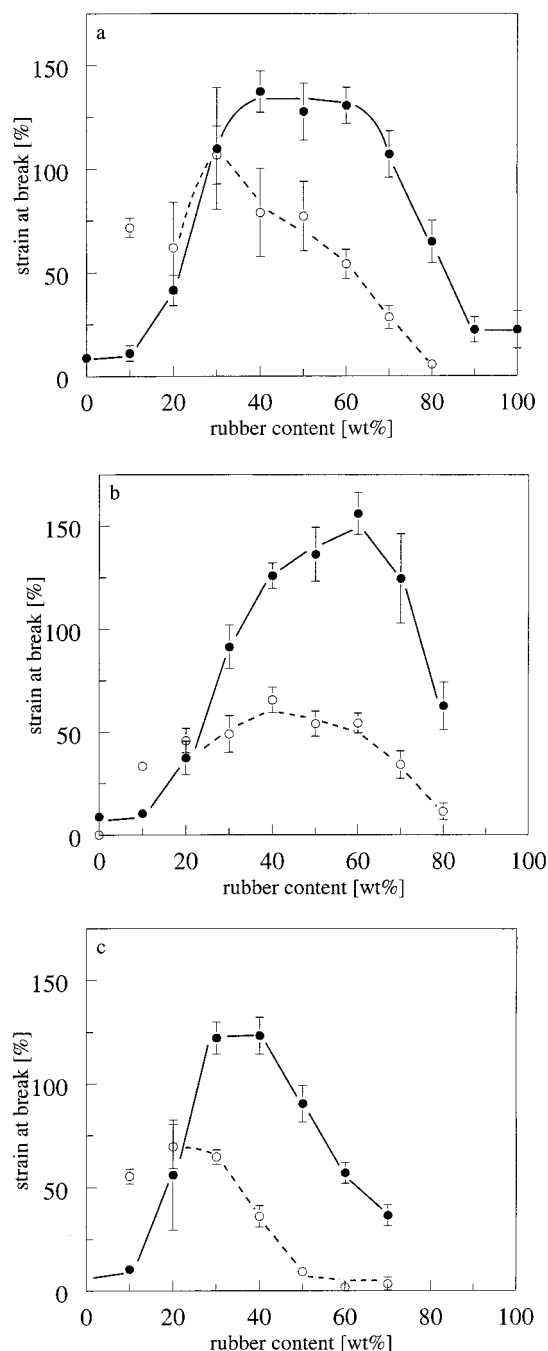


Figure 4. Macroscopic (●) and plastic (○) strain at break of the PMMA/epoxy systems: (a) semi-IPN; (b) full-IPN; (c) GMA copolymer.

perpendicular direction, which suggests the absence of craze fibrils or the formation of crazes with a limited amount of fibrils.

For the 80/20 full-IPN, deformation does not result in the elliptically shaped scattering pattern as observed for the semi-IPN, which indicates the absence of voids being elongated in the tensile direction; see Figure 8e. Moreover, cavitation seems to be suppressed as can be concluded from the limited changes in the scattered intensity during drawing, not shown here. This is confirmed by the macroscopic tensile tests which, in contrast to the semi-IPN, do not show any stress-whitening. Instead, some additional scattering in the tensile direction is found. Although not fully understood, this may be the result of the initiation of a limited amount of crazes or cracklike voids.² The combination

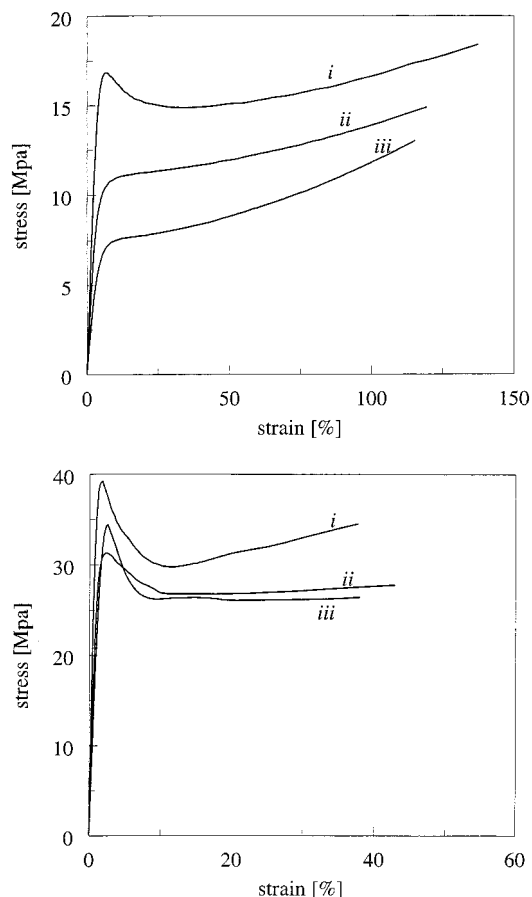


Figure 5. Stress-strain curves for the three PMMA/epoxy blends: (i) semi-IPN; (ii) full-IPN; (iii) GMA copolymer at two compositions, (a) 60/40 and (b) 80/20.

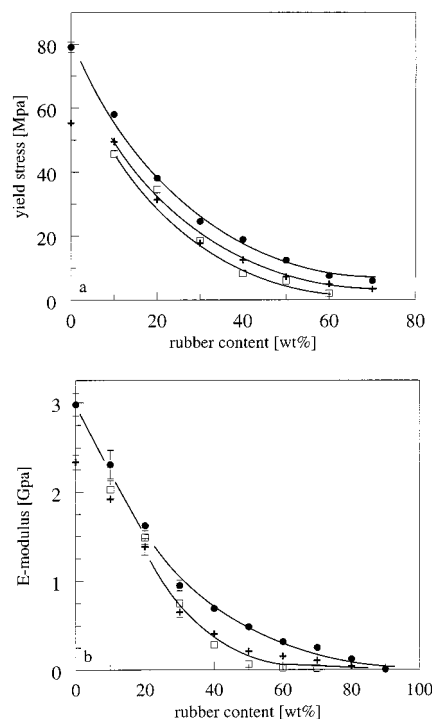


Figure 6. (a) Yield stress and (b) modulus of (●) semi-IPN, (□) full-IPN, and (+) GMA copolymer.

with the weak scattering at the equator results in a pattern rather similar to that of the 70/30 semi-IPN which was explained in terms of morphological orientation. For the 80/20 full-IPN, the equator scattering is,

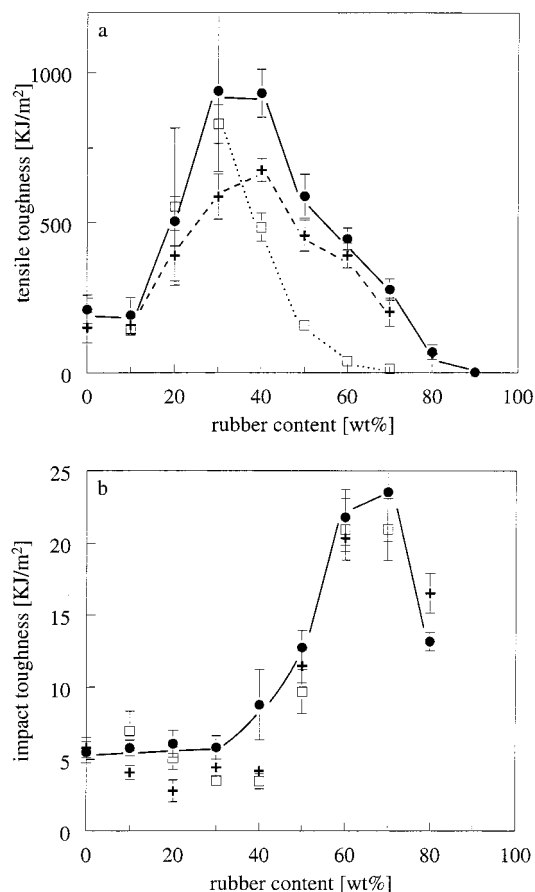


Figure 7. (a) Tensile and (b) impact toughness of (●) semi-IPN, (□) full-IPN, and (+) GMA copolymer.

however, considerably less, which may be the result of the cross-linked PMMA phase suppressing the morphological orientation.

The resulting scattering pattern of the 70/30 full-IPN as shown in Figure 8f has not been observed earlier, and a possible explanation for the scattering pattern will be given below. The scattering perpendicular to the tensile direction is again similar to that of the 70/30 semi-IPN and may again be caused by the orientation of the morphology. This, however, cannot explain the additional scattering in the tensile direction. A possible alternative reason is the localization of deformation which results in zones in the order of tens of nanometers possessing a different electron density. This may result in the scattering pattern observed if these zones are asymmetrically shaped and positioned in such a way that their average distance is smaller in the tensile direction.

3.5.3. Copolymer. As can be concluded from the first scattering pattern in Figure 8g, the 90/10 composition of the copolymer also deforms via crazing. As observed for the full-IPN with the same composition, the scattering streak in the tensile direction is sharper in comparison to the 90/10 semi-IPN. Moreover, the pattern does not show any scattering resulting from possible craze fibrils.

In contrast, tensile deformation of the 80/20 copolymer system results in the typical cross-shaped craze scattering pattern, Figure 8h, including the scattering in the perpendicular direction which is relatively strong in comparison to the 90/10 semi-IPN. Considering the cross-linked character of the system and the craze pattern of the 90/10 composition, the development of

crazes with a high fibril content may be rather unexpected. The sharp streaks in the tensile direction, however, do suggest that this system indeed deforms via crazing. Remarkably, the scattering angle in the perpendicular direction is considerably larger in comparison to the craze scattering patterns discussed earlier. For crazes in polycarbonate at elevated temperatures,²³ comparable scattering patterns have been observed where the large scattering angle is ascribed to the relatively thicker craze fibrils in comparison to polystyrene and poly(methyl methacrylate). A second possible explanation may be a wide distribution of interfibril distances. In conclusion, the results suggest that deformation of the 80/20 copolymer system is mainly accompanied by crazing.

The scattering pattern of the 70/30 copolymer system, Figure 8i, does not show any evidence of dilatation processes and/or orientation. Apparently, deformation of the thermosetting network occurs rather homogeneously without the introduction of any electron density differences. Hence, shear yielding is the only mode of microscopic deformation involved.

3.6. Macroscopic vs Microscopic Deformation.

According to the results presented, the macroscopic properties are scarcely influenced by the degree of demixing. The mode of microscopic deformation, however, clearly changes for the different systems within the composition range studied. The brittle blends containing 10 wt % epoxy resin all deform via crazing while for the 80/20 composition significant differences are observed. Although the macroscopic toughness is the same, the semi-IPN 80/20 is the only system which clearly shows cavitation while the copolymer system again deforms by craze formation. Apparently, the toughness enhancement in the latter case is the result of multiple crazing. After all, this may not be surprising since cavitation is not very likely to occur in the homogeneous system. Finally, the enhanced tensile toughness of the 70/30 systems is in all cases accompanied by the occurrence of shear yielding without any dilatation processes. However, the differences in both morphology and network give rise to changing scattering patterns.

4. Conclusions

In this study, it has been demonstrated that the degree of phase separation in the PMMA/epoxy semi-IPN systems can be reduced by cross-linking the PMMA phase, which results in the formation of full-IPNs, or by the partial copolymerization of both phases. A comparable synergistic toughening effect is observed for all three systems under both tensile and impact conditions. Generally, the difference in mechanical behavior between the three systems is surprisingly limited. For the intermediate compositions (30–60 wt % rubber), however, the tensile toughness of the semi-IPNs is clearly higher, which is most likely the result of an enhanced degree of demixing.

It remains, however, difficult to distinguish unambiguously between the separate effects of interphase mixing and morphology on the mechanical behavior. Interestingly, compared to the pure copolymer with its broad spectrum in compositions all with their own T_g , the full- and semi-IPNs demonstrate a toughness equal or even higher than that of the copolymer system. For this reason interphase mixing alone cannot be responsible for the toughness improvement. In the line of the

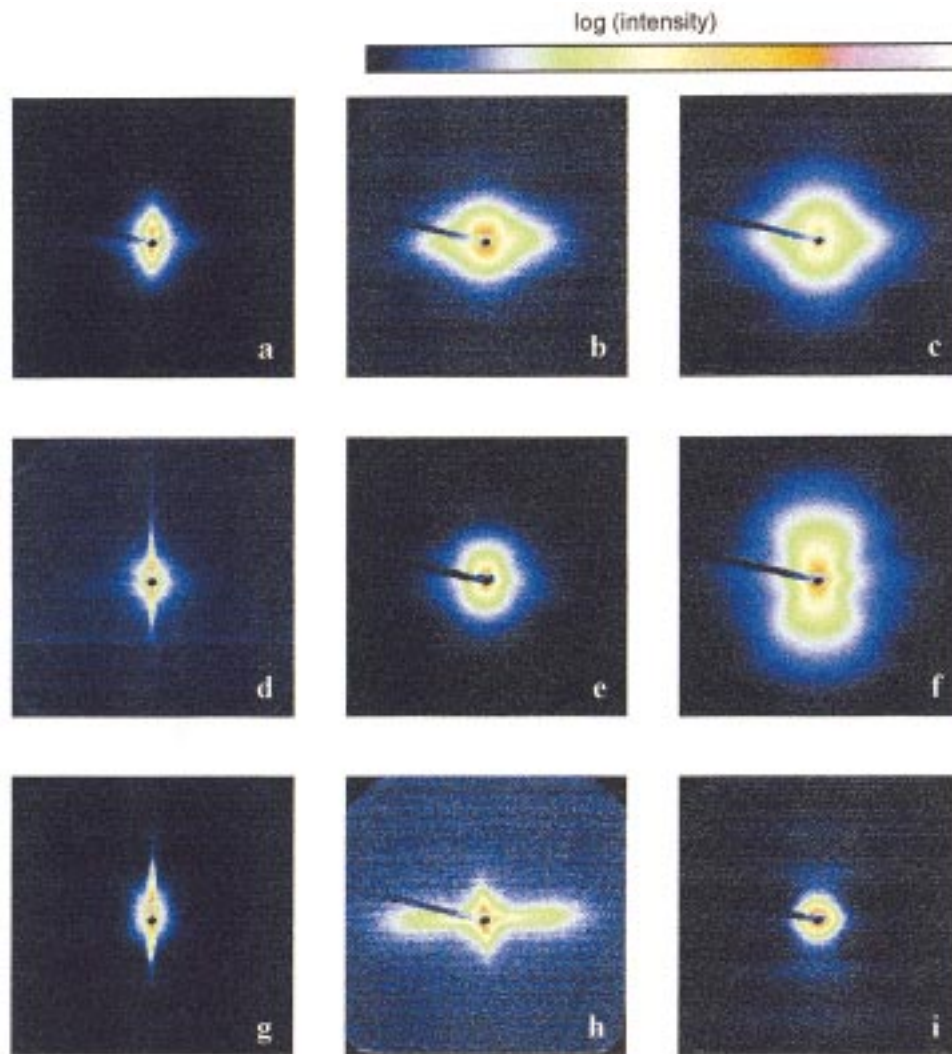


Figure 8. SAXS patterns prior to fracture of PMMA/epoxy systems: semi-IPNs (a) 90/10, (b) 80/20, and (c) 70/30; (d–f) same composition for full-IPNs; (g–i) same compositions for copolymers. Tensile direction is vertical. Experiments were performed at ESRF, ID2-BL4. In the setup used, the maximum and minimum d values recorded on the two-dimensional detector were 150 and 10 nm, respectively.

experimental results reported in this series,^{1–3} the nanometer-sized morphology realized can cause a transition in mode of microscopic deformation from crazing to complete shear yielding,^{1,4,5} even—via precavitation—at impact rates for compositions with a low volume fraction of rubber.

Acknowledgment. The authors are grateful for availability of the beamline ID2/BL4 at the European Synchrotron Radiation Facility (ESRF, Grenoble, France). Dr V. Narayan is acknowledged for his experimental support together with the assistance of Dr. A. Hammersley in the analysis of the data with the help of the FIT2D software program, developed at the ESRF.

References and Notes

- (1) Part 1: Jansen, B. J. P.; Meijer, H. E. H.; Lemstra, P. J. *Polymer*, submitted for publication.
- (2) Part 2: Jansen, B. J. P.; Rastogi, S.; Meijer, H. E. H.; Lemstra, P. J. *Macromolecules*, submitted for publication.
- (3) Part 3: Jansen, B. J. P.; Rastogi, S.; Meijer, H. E. H.; Lemstra, P. J. *Macromolecules*, **1999**, *32*, 6283.
- (4) Smit, R. J. M.; Meijer, H. E. H.; Brekelmans, W. A. M.; Govaert, L. E. *J. Mater. Sci.*, submitted for publication.
- (5) Sanden van der, M. C. M.; Meijer, H. E. H.; Lemstra, P. J. *Polymer* **1993**, *34*, 10, 2148.
- (6) Jansen, B. J. P.; Meijer, H. E. H.; Lemstra, P. J., *Polymer* **1999**, *40*, 2917.
- (7) Klempner, D.; Sperling, L. H.; Utracki, L. A. *Advances in Chemistry*; American Chemical Society: Washington, DC, 1994; Vol. 239.
- (8) Kim, S. C.; Sperling, L. H. *IPNs around the world*; John Wiley & Sons: Chichester, England, 1997.
- (9) Sperling, L. H.; Mishra, V. In *IPNs around the world*; Kim, S. C., Sperling, L. H., Eds.; John Wiley & Sons: Chichester, England, 1997; p 1.
- (10) Mishra, V.; Du Prez, F. E.; Gosen, E.; Goethals, E. J.; Sperling, L. H. *J. Appl. Polym. Sci.* **1995**, *58*, 331.
- (11) Chen, Q.; Ge, H.; Chen, D.; He, X.; Yu, X. *J. Appl. Polym. Sci.* **1994**, *54*, 1191.
- (12) Akay, M.; Rollins, S. N. *Polymer* **1993**, *34*, 9, 1865.
- (13) Akay, M.; Rollins, S. N.; Riordan, E. *Polymer* **1988**, *29*, 37.
- (14) Chou, Y. C.; Lee, L. J. *Polym. Eng. Sci.* **1995**, *35*, 12, 976.
- (15) Han, X.; Chen, B.; Guo, F. In *IPNs around the world*; Kim, S. C., Sperling, L. H., Eds.; John Wiley & Sons: Chichester, England, 1997; p 241.
- (16) Hourston, D. J.; Schäffer, F. U. *Polymer* **1996**, *37*, 16, 3521.
- (17) Gilmer, T. C.; Hall, P. K.; Ehrenfeld, H.; Wilson, K.; Bivens, T.; Clay, D.; Emdreszl, C. *J. Polym. Sci., Polym. Chem. Ed.* **1996**, *34*, 1026.
- (18) Barret, L. W.; Sperling, L. H.; Gilmer, J. W.; Mylonakis, S. G. In *Advances in Chemistry*; Klempner, D., Sperling, L. H., Utracki, L. A., Eds.; American Chemical Society: Washington, DC, 1994; Vol. 239, p 489.
- (19) Jang, B. Z.; Pater, R. H.; Soucek, M. D.; Hinkley, J. A. *J. Polym. Sci., Part B: Polym. Phys. Ed.* **1992**, *30*, 643.

- (20) Venderbosch, R. W.; Meijer, H. E. H.; Lemstra, P. J. *Polymer* **1994**, 33, 4349.
- (21) Park, J. W.; Kim, S. C. In *IPNs around the world*; Kim, S. C., Sperling, L. H., Eds.; John Wiley & Sons: Chichester, England, 1997; p 27.
- (22) Scarito, P. R.; Sperling, L. H. *Polym. Eng. Sci.* **1979**, 36, 297.
- (23) Bark, M.; Cunis, S.; Fink, M.; Gehrke, R.; Heise, B.; Karl, A.; von Krosigk, G.; Lode, U.; Pomper, T.; Wilke W. *Tagungsband "Polymerwerkstoffe '96"* **1996**, 350.

MA981407F